Journal of Electroanalytical Chemistry 759 (2015) 8–13

Contents lists available at ScienceDirect

Journal of Electroanalytical Chemistry

journal homepage: www.elsevier.com/locate/jelechem

Carbon nitride nanosheets sensitized quantum dots as photocathode for photoelectrochemical biosensing

Qing Hao, Jianping Lei *, Quanbo Wang, Yang Zang, Huangxian Ju

State Key Laboratory of Analytical Chemistry for Life Science, School of Chemistry and Chemical Engineering, Nanjing University, Nanjing 210093, PR China

ARTICLE INFO

Article history:
Received 31 January 2015
Received in revised form 28 April 2015
Accepted 1 May 2015
Available online 15 May 2015

Keywords:
Photoelectrochemistry
Quantum dots
Carbon nitride nanosheets
Biosensors
Detection
Signal amplification

ABSTRACT

A highly efficient photocathode, based on graphite-like carbon nitride nanosheets (CNNS) sensitized CdTe quantum dots (QDs), was constructed for photoelectrochemical (PEC) biosensing. Using dissolved oxygen as an electron acceptor, the hybrid photocathode showed a sensitive photocurrent response at −0.2 V bias potential under 405 nm illumination. The CdTe/CNNS hybrid photocathode demonstrates about 100% increase of photocurrent compared to CdTe QDs modified electrode owing to the formation of heterojunction through contact of two semiconductor materials. The improved charge separation efficiency was identified by the extension of electron transit time (τ_d) and electron lifetime (τ_n) in this PEC system. The introduction of Cu^{2+} on the surface of hybrid photocathode could decrease photocurrent via the exciton trapping quenching effect. A sensitive PEC sensor for Cu^{2+} was thus developed with a good linear range from 20 nM to 100 μM and a detection limit of 3.3 nM, and was successfully applied in the detection of Cu^{2+} in human hair samples. The CNNS-sensitized photocathode provides a good alternative for enhancement of the PEC signal transduction and could be widely used in biosensing and clinical diagnosis.

1. Introduction

Photoelectrochemical (PEC) technique, as a novel strategy integrating electrochemistry with photochemistry, has attracted growing attention in various areas such as photovoltaic devices, photocatalysis and bioanalysis [1–3]. The PEC strategy has exhibited a large number of unique advantages such as low bias potential, high sensitivity and low background owing to the separation of excitation signal (light) and detection signal (current) [4]. Various photoelectrochemical biosensors have been designed based on organic materials [5], metal oxide semiconductor [6], quantum dots [7,8], and hybrid materials [9] for the detection of metal ions [10], biomolecules [11], and even cells [12]. For the amplification strategy of PEC, the hybrid materials provide an efficient way to improve the charge separation efficiency due to the synergic effect among their components. In particular, the assembly of dye-sensitized semiconductor is a kind of strategy to amplify PEC signal [13]. Meanwhile, the incorporation of noble metal nanoparticles has been discovered for enhancing the photoconversion efficiency of TiO_2 via surface plasmon resonance [14,15]. Here, in order to further improve the photoelectrochemical conversion efficiency, the carbon nitride nanosheets are introduced to sensitize quantum dots as a photocathode for enhancing the PEC activity.

As a medium band gap and metal-free indirect semiconductor material, graphite-like carbon nitride (g-C_3N_4) simply prepared by polymerization of melamine possesses well electrical and optical properties, and excellent stability [16]. Conventionally, the bulk and mesoporous g-C_3N_4 have been applied in the areas of photoluminescence detection, photocatalysis, photodegradation and photovoltaic device [17–22]. Recently, the exfoliated g-C_3N_4 nanosheets (CNNS) with a band gap of 2.7 eV was found to be chemically reactive and exhibit excellently photocatalytic activity [23–26]. More interestingly, combining CNNS substrates with supported metal nanoparticles could result in controlled access to metal−semiconductor heterojunction and enhanced electron transfer between photoexcited semiconductor and gold nanoparticles [27]. Therefore, it is rational to design a PEC sensing platform by using CNNS as supporter to contact with QDs, in which the injection of electrons might mediate from QDs into CNNS conduction band (CB) by heterojunction, and improve the photoinduced charge separation, thus leading to the enhanced photocurrent for PEC biosensing.

Using copper ions (Cu^{2+}) as a model analyte, the PEC behavior and application potential of this CNNS/CdTe hybrid photocathode was evaluated through the quenching effect of Cu^{2+} on the photocurrent. Copper is an essential trace element for humans, which acts as key element for activities in some important proteins. However, excess Cu^{2+} ions become harmful to humans' body [28]. Therefore, it's necessary to develop reliable and sensitive detection strategy of Cu^{2+}. In this work, a hybrid photocathode was constructed based on CNNS sensitized CdTe QDs as PEC materials via stepwise modified method (Scheme 1). The heterojunction between CNNS and CdTe was formed through stacking and contacting of two semiconductor layers, in

* Corresponding author.
E-mail address: jpl@nju.edu.cn (J. Lei).

http://dx.doi.org/10.1016/j.jelechem.2015.05.001
1572-6657/

which the Femi energy of CdTe and CNNS adjust to suit each other, and reach the equilibrium, thus resulting in the high efficiency of charge separation. The CdTe/CNNS hybrid photocathode demonstrates about 100% increase of photocurrent compared to CdTe QDs modified electrode. The introduction of Cu^{2+} onto hybrid photocathode generated exciton-traps, which inhibited the generation of photocurrent [29]. The quenching photocurrent of CdTe/CNNS photocathode is utilized for the sensitive and selective detection of Cu^{2+} with a 4-order linear range and a detection limit low to nanomole, and has been successfully applied in detection of Cu^{2+} in human hair samples, showing the potential applications in practice.

2. Materials and methods

2.1. Materials and reagents

Cadmium chloride ($CdCl_2 \cdot 2.5H_2O$) was purchased from Alfa Aesar China Ltd. Tellurium powder and sodium borohydride were purchased from Sinopharm Chemical Reagent Co. Ltd. Cupric nitrate ($Cu(NO_3)_2 \cdot 3H_2O$) was purchased from Shanghai Sinpeuo Fine Chemical Co. Ltd. (China). Melamine and 3-mercaptopropionic acid (MPA, ≥99%) were purchased from Sigma–Aldrich (China) and used as supplied. All other chemicals were of analytical grade without further purification. Tris–HCl buffer (10 mM, containing 0.1 M NaCl as supporting electrolyte, pH 7.0) was employed as PEC electrolyte during the photoelectrochemical procedure. Indium tin oxide (ITO) coated glass as the electrode material was purchased from Zhuhai Kaivo Electronic Components Co. Ltd. The ultrapure water (≥18 MΩ, Milli-Q, Millipore) was used throughout the experiment.

2.2. Apparatus

Cyclic voltammetric experiments were performed on a CHI 660D electrochemical workstation (CH Instruments Inc., USA). X-ray photoelectron spectroscopy (XPS) experiments were operated on an ESCALAB 250 spectrometer (Thermo-VG Scientific Co., USA) with an ultrahigh vacuum generator. The UV–Vis absorption spectra were obtained with a UV-3600 UV–Vis–NIR spectrophotometer (Shimadzu Co., Kyoto, Japan). The scanning electron microscopic (SEM) images were obtained by Hitachi S-4800 scanning electron microscope (Japan). The transmission electron micrograph (TEM) was obtained using a JEM-2100 TEM instrument (JEOL, Japan). Photoelectrochemical measurements were detected on a Zahner intensity modulated photo Spectrometer (Zahner Zennium, German) with a LW405 LED light (wavelength at 405 nm) as the light source. All modified processes were performed under 37 °C, and all PEC experiments were carried out at room temperature using a conventional three-electrode system, with a modified ITO electrode, a platinum wire and a saturated calomel electrode as working, counter and reference electrodes, respectively.

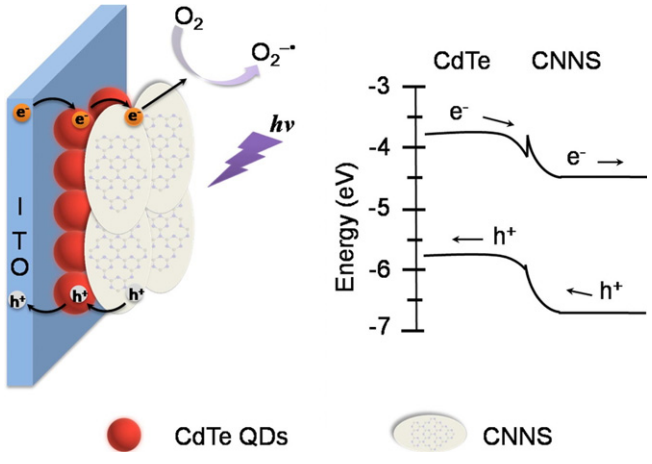

Scheme 1. Schematic illustration of the photoelectrochemical mechanism through the formation of heterojunction, and the energy levels of CdTe/CNNS hybrid photocathode.

2.3. Preparation of MPA-CdTe QDs

The synthesis of CdTe QDs was refered to the method reported for thiol-capped CdTe QDs in aqueous phase [30]. First, the Cd precursor solution was prepared by mixing 26 μL of MPA (~6 mM) solution with 50 mL of 2.0 mM $CdCl_2$ solution. After adjusted to pH 9.0 with 1 M NaOH, 0.80 mL of 0.0625 M N_2-saturated NaHTe solution was injected under a N_2 atmosphere and vigorous stirring. The resulting mixture solution was heated to 99–100 °C and refluxed for around 10 h to obtain the MPA-CdTe QDs. Then 900 μL as-prepared QDs solution was mixed with the same amount of isopropanol. The colloidal precipitate was collected by centrifugation (6000 rpm, 5 min) to remove excess reactants, and redispersed with ultrapure water. The CdTe QDs solution was keeped at 4 °C before use.

2.4. Synthesis of C_3N_4 nanosheets

The C_3N_4 nanosheets (CNNS) were synthesized from bulk graphitic-phase carbon nitride (g-C_3N_4) liquid exfoliation route in water according to literature [31]. First, the g-C_3N_4 was synthesized by polymerization of melamine. Then 100 mg bulk g-C_3N_4 powder was added into 100 mL water, and kept ultrasonication for 16 h to dissolve the g-C_3N_4 precipitate. The well-distributed CNNS was centrifuged at 5000 rmp for 20 min to remove the excess bulk g-C_3N_4 and large size of g-C_3N_4 nanoparticles and nanosheets, which offered a pretty uniform size for the construction of PEC sensors. The as-prepared CNNS solution was stored at room temperature.

2.5. Construction and Cu^{2+} detection of PEC sensor

An ITO glass was cut into 4.5 cm × 0.8 cm slices to suit for PEC detection. ITO slices were cleaned by bathing in 0.5 M NaOH and 10% H_2O_2 for 10 min, sequentially. After bathed in acetone for another 30 min, the slices were washed by ultrapure water, and then dried at 37 °C. 10 μL as-prepared CdTe QDs solution was dropped onto the ITO electrode and dried at 37 °C to obtain CdTe QDs modified electrode. Then the CdTe QDs modified electrode was coated by certain concentration CNNS, and dried at 37 °C to construct the CdTe/CNNS photocathode. The hybrid photocathode was used as the working electrode for PEC detection. For Cu^{2+} detection, 10 μL certain concentration Cu^{2+} standard stock solution was dropped onto a working electrode, following dried at room temperature. After constructing the photocathode, the whole assay can be achieved in 15 min.

The time-dependent photocurrent, intensity-modulated photocurrent spectroscopy (IMPS) and intensity-modulated photovoltage spectroscopy (IMVS) measurements were performed under light excitation of 405 nm in 10 mM Tris–HCl solution containing 0.1 M NaCl. The intensity of light source was based on specific situation increasing from 10 to 150 W m^{-2}.

The human hair sample was digested with the mixture of 70% (W/W) nitric acid and 60% (W/W) perchloric acid (3:1 V/V). The as-prepared sample solution was diluted and neutralized to pH 6 with 1 M NaOH solution before use. The human hair sample was analyzed in a manner similar to that described above.

3. Results and discussion

3.1. Characterization of CNNS and QDs

The well-distributed CNNS was synthesized by a "green" liquid exfoliation route from bulkg-C_3N_4. The average diameter of CNNS measured from the TEM images is around 100 nm (Fig. 1A). Meanwhile, the UV–

Vis spectrum of as prepared CNNS showed an absorption band in centered at around 316 nm (Fig. 1B, curve a), which is attributed to its' intrinsic absorption edge and could be a basis of calculating the band gap (~2.7 eV) of CNNS [31]. These typical characteristic indicates the successful preparation of CNNS, and the good dispersibility is favorable for constructing biosensing platform.

CdTe QDs shows a wide absorption band with an absorption peaks at 565 nm in UV–Vis spectrum (Fig. 1B, curve b). According to the Peng's empirical equation [32], the diameter and concentration of the redispersed QDs solution was estimated to be 3.4 nm and 1.5 μM, respectively. Combining with the redox couple of QDs modified ITO electrode (Fig. 2A), the energy levels of CB and valence band (VB) of QDs are determined as around 3.65 eV and 5.60 eV, respectively [33]. Based on the appropriate band alignment between CdTe QDs and CNNS, the CdTe/CNNS photocathode was constructed for the following experiments.

3.2. SEM morphology of photocathode

The SEM images of CdTe QDs modified electrode show a uniform distribution of QDs on the ITO electrode (Fig. 1C), while porous nanosheets structure were observed on the CdTe/CNNS photocathode (Fig. 1D). The cross-sectional SEM image for the CdTe/CNNS photocathode shows that the thickness of the CdTe QDs and CNNS layer is 294 ± 2.5 nm and 130 ± 2.8 nm, respectively (Fig. 1D, inset). These data identified well construction of hybrid photocathode via the stepwise fabrication.

3.3. PEC behaviors of photocathode

Fig. 2B depicts the photocurrent responses of CdTe/CNNS photocathode (Fig. 2B, curve a) and CdTe QDs modified electrode (Fig. 2B, curve b). Under 405 nm light irradiation, the CdTe QDs modified electrode generated a photocurrent around 750 nA through charge separation of electron–hole pairs. After hybridizing with CNNS, around 100% improvement of photocurrent was detected in the CdTe/CNNS photocathode system. This should be attributed to the formation of heterojunction between the two materials, which could force photo-generated electrons and holes moving in the opposite direction to avoid charge recombination, thus improving the charge separation efficiency [34].

Considering the energy levels of CdTe QDs and CNNS [16], the heterojunction structure on the surface of hybrid photocathode was confirmed by the current–voltage (*I–V*) curves. The appearance of electrical breakdown in *I–V* curve of photocathode is the typical characteristic for the formation of heterojunction (Fig. 2C). To further understand the improvement of photocurrent, IMPS and IMVS experiments have been employed to evaluate the electron transit time (τ_d) and electron lifetime (τ_n) of both CdTe QDs modified electrode and CdTe/CNNS photocathode (Fig. 2D). By applying a perturbation signal on the light source, the τ_d and τ_n were calculated by the expression $\tau_d = (1/2)\pi f_{IMPS}$, and $\tau_n = (1/2)\pi f_{IMVS}$ (the f is the frequency of the minimum IMPS and IMVS imaginary component), respectively [35]. As shown in Fig. 2D, with the light intensity increasing from 10 to 150 W m^{-2}, the τ_d decreased and had negative correlation with light intensity. The τ_d of the CdTe/CNNS photocathode (about 0.8−1.2 ms) under different light intensity is shorter than that of the CdTe QDs modified electrode (about 1.0−1.4 ms), which is attributed to the formation of heterojunction, thus leading to a considerable improvement of photocurrent. Meanwhile, the τ_n, which characterizes the recombination processes of electrode, was measured by IMVS under 100 W m^{-2}. The average lifetime (Fig. 2D, inset) of CdTe/CNNS photocathode (115.4 ms) was longer than that of the CdTe QDs modified electrode (78.3 ms), confirming that the recombination process was inhibited by the formation of heterojunction. The high efficiency of charge separation significantly increased the PEC behavior of hybrid photocathode.

3.4. Quenching mechanism of Cu^{2+}

The photocurrent of the PEC system was quenched obviously, when Cu^{2+} was introduced onto the CdTe/CNNS photocathode surface (Fig. 2B, curve c). Considering that the sedimentation equilibrium constant of CuS (8×10^{-36}) is much smaller than that of CdS (7×10^{-27}), S atoms on the surface of CdTe could strongly adsorbed Cu^{2+}. The XPS spectrum of $Cu2p_{3/2}$ on the hybrid photocathode incubated with 0.1 mM Cu^{2+} showed the interaction between Cu and S atoms on the surface of CdTe. The binding energy of $Cu2p_{3/2}$ splits into three parts with peak values of 931.4, 932.3 and 933.3 eV (Fig. 3A), which represented the existence of Cu^{I}, Cu_xS at the mixed valence state, and Cu^{2+}, respectively. The redox energy level of Cu^{I} took place between VB and CB of the QDs, resulting in the formation of the trapping sites [29], and thus decreasing the cathode photocurrent response. Meanwhile, the binding energy of N1s splits into 398.5 (C—N═C), 399.0, 399.6 (N—C_3), 400.7 (C—N—H) and 401.5 eV on the surface of hybrid photocathode (Fig. 3B). The presence of 399.0 and 401.5 eV could be attributed to complex formation between Cu^{2+} and amino/imino functions of CNNS [20], and thus photoinduced electron transfer (PET) should occur from the CB of CNNS to the complexed Cu^{2+} [36]. Therefore, the quenching effect is attributed to the exciton trapping produced on the surface of CdTe QDs and PET process between CNNS and Cu^{2+}, providing the feasibility for sensitive determination of Cu^{2+}.

3.5. Optimization of detection conditions

To obtain the good performance, the following experiments were carried out to optimize the several key parameters. Firstly, the pH of electrolyte significantly influenced the PEC behavior of photocathode (Fig. 4A). In the examined pH range, with the pH increasing from 6.0 to 9.0, the photocurrent decreased. Considering the slight difference of photocurrent between pH 6.0 and 7.0, and further application in physiological conditions, pH 7.0 HCl–Tris buffer was chose as the electrolyte. The light intensity is other important parameter for photocurrent intensity (Fig. 4B). The photocurrent increased with the light intensity increasing from 55 to 130 W m^{-2}. Taking into account the photocurrent under 100 W m^{-2} was large enough to construct biosensor, and the energy saving and biocompatibility, we chose 100 W m^{-2} as the detection light intensity. Also, the photocurrent depended on the concentration of CNNS modified on the electrode (Fig. 4C). The PEC behavior of hybrid photocathode reached a maximum value when the concentration of CNNS is at 1 mg mL^{-1}. Therefore, 1 mg mL^{-1} was chosen as the experimental concentration.

3.6. PEC detection of Cu^{2+}

Under the optimal conditions, the CdTe/CNNS photocathode was used to establish a PEC sensor for Cu^{2+} (Fig. 5A). Photocurrent (I_p) decreased with the concentration of Cu^{2+} increasing, and the calibration plot showed a good linear relationship between the quenching coefficient (I_p/I_0) and the logarithm value of Cu^{2+} concentration in a range of 20 nM to 100 μM (Fig. 5B). The linear equation was calculated to be $I_p/I_0 = -0.87 - 0.24 \log c$ with a correlation coefficient of 0.990. The detection limit was calculated as 3.3 nM at 3σ, which was lower than ZnO/CdS hierarchical nanosphere based anodic PEC sensor [37]. The low detection limit and wide linear range of the proposed PEC sensor may be attributed to the low background from separation of excitation and detection signals, and the dual quenching effect of Cu^{2+} on the hybrid photocathode.

3.7. Stability of PEC biosensor

The stability of PEC biosensor was investigated by eight measurements of photocurrent peaks, through turning light source on and off, in the absence and presence of 50 μM Cu^{2+} (Fig. 6). The

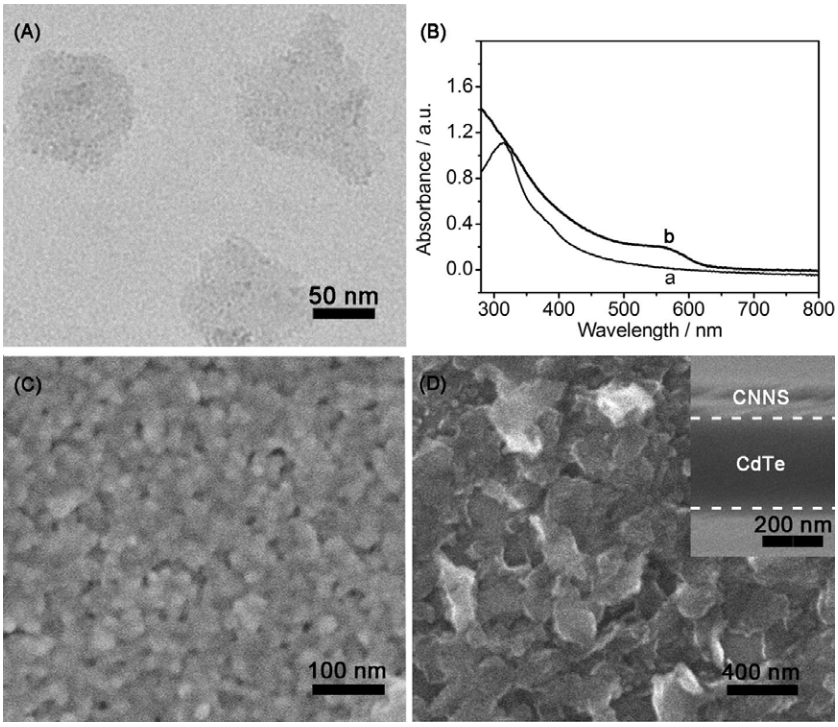

Fig. 1. (A) TEM image of CNNS, (B) UV–Vis absorption spectra of 1 mg mL^{-1} CNNS (a) and as-prepared QDs (b), SEM images of (C) CdTe QDs modified electrode, and (D) CdTe/CNNS hybrid photocathode. Inset: Cross-sectional SEM image of CdTe/CNNS photocathode.

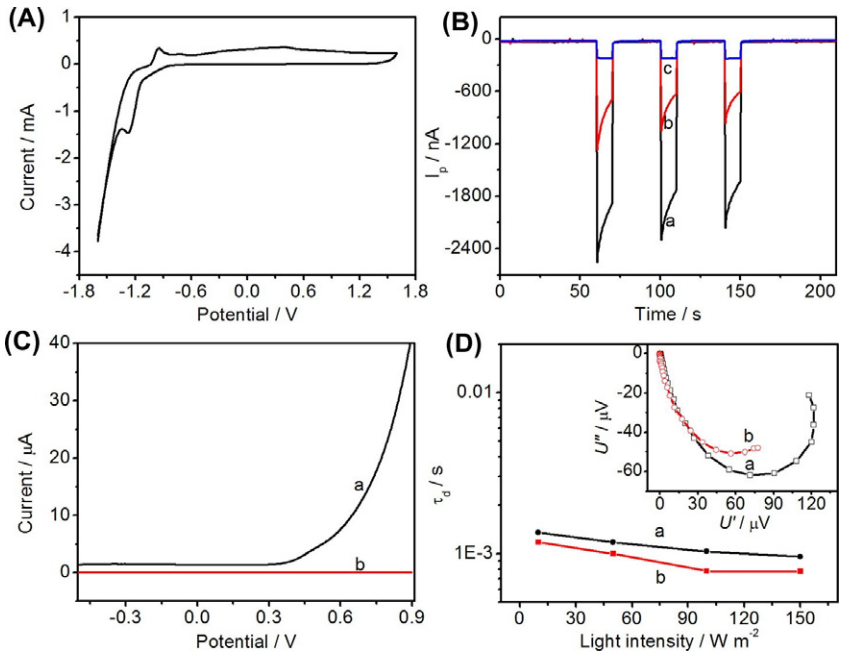

Fig. 2. (A) Cyclic voltammetries in N_2-saturated PBS at CdTe QDs modified electrode, Scan rate: 100 mV s^{-1}. (B) Photocurrent of CdTe/CNNS hybrid photocathode (a), CdTe QDs modified electrode (b) and hybrid photocathode incubated with 0.1 mM Cu^{2+} (c) in air-saturated PBS. (C) *I–V* curves of CdTe/CNNS photocathode (a) and CdTe QDs modified electrode (b) in air-saturated PBS. (D) Dependence of the electron transit time, τ_d of CdTe QDs modified electrode (a) and CdTe/CNNS photocathode (b) under 10, 50, 100, 150 W m^{-2} measured by IMPS measurement. Inset: IMVS imaginary component under 100 W m^{-2} of CdTe QDs modified electrode (a) and CdTe/CNNS photocathode (b).

relative standard deviations (RSDs) were 1.7% and 1.8%, which indicated acceptable stability and reliability of the PEC sensor. Meanwhile, the inter-assay precision of five photocathodes was examined at 50 μM Cu^{2+}, and RSD of the five measurements was 4.7%, showing the acceptable fabrication reproducibility. Furthermore, the photocurrent of photocathode decreased to 91.5± 3.0% after storage at 4 °C in air condition for 15 days, showed good storage stability.

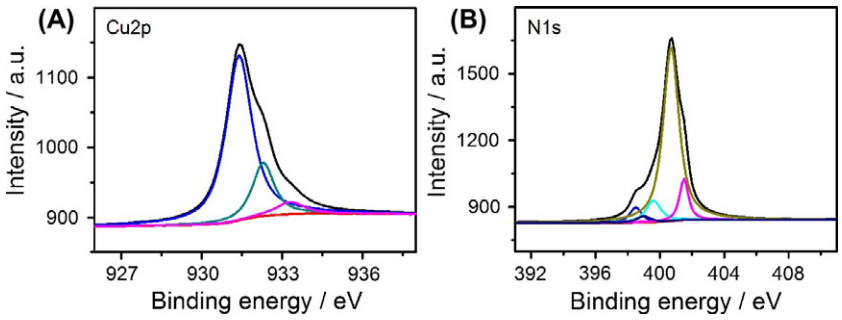

Fig. 3. (A) Cu2p and (B) N1s XPS spectra of CdTe/CNNS incubated with 0.1 mM Cu^{2+}.

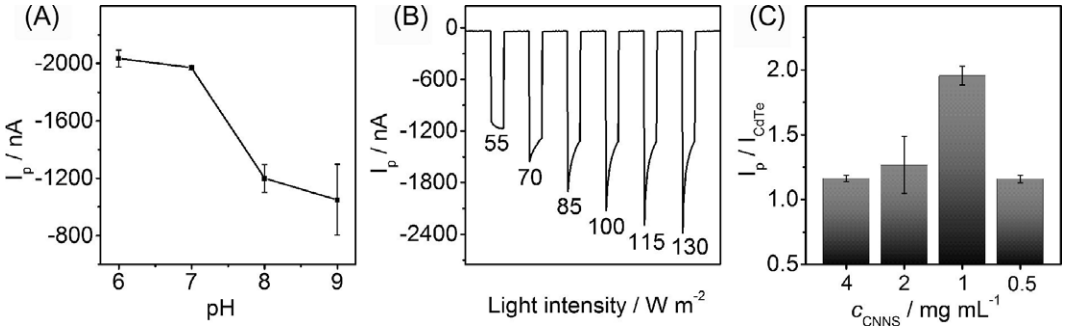

Fig. 4. Effects of (A) pH of detection solution, (B) light intensity of light source, (C) concentration of CNNS on the PEC responses.

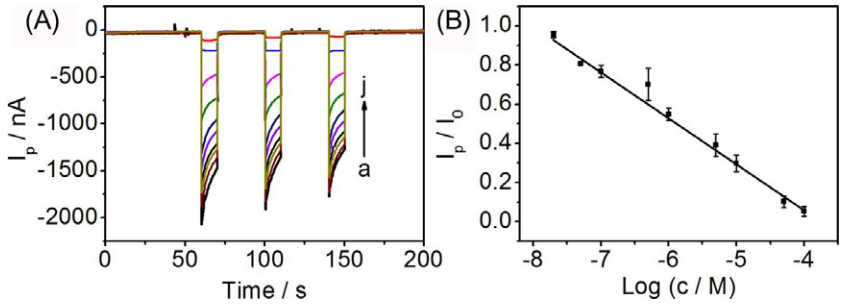

Fig. 5. (A) Photocurrent of the optimized PEC sensor in response to different concentrations of Cu^{2+}: 0, 0.02, 0.05, 0.1, 0.5, 1.0, 5.0, 10, 50 and 100 μM (from a to j). (B) Plot of ECL intensity *vs* logarithm value of Cu^{2+} concentration.

3.8. Selectivity of PEC biosensor

To further study the selectivity of proposed PEC biosensor, some cations such as Mn^{2+}, Mg^{2+}, Co^{2+}, Fe^{3+}, Hg^{2+}, Ni^{2+}, Cd^{2+} and Pb^{2+} were chosen as interferences, and the photocurrent was detected under the same conditions (Fig. 7). No significant response was observed at 10 μM of those interferences compared to the same concentration of Cu^{2+}, indicating a good ability of anti-interference for Cu^{2+} detection.

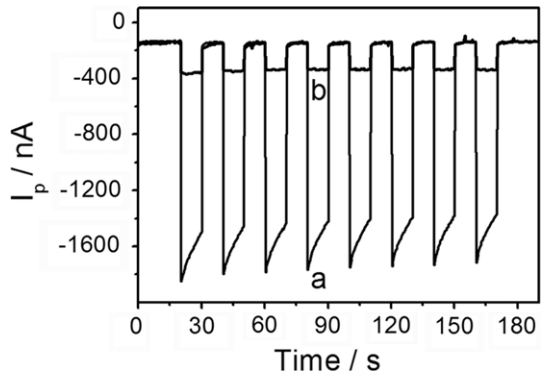

Fig. 6. Stability of hybrid photocathode before (a) and after (b) incubated with 50 μM Cu^{2+}.

3.9. Application in human hair sample

In order to evaluate the prospects of proposed strategy, the present PEC sensor was applied to detect Cu element in a human hair sample. The copper element content detected through our method was 12.6 μg g^{-1}, which was close to the value of 10.1 μg g^{-1} obtained from inductively coupled plasma spectrometry. When spiked with 3 μM, 6 μM and 12 μM Cu^{2+} standard solution, the recoveries was detected to be 92.3 ± 13.9%, 103.2 ± 4.3% and 92.2 ± 2.4%. The experiment result indicated the good precision of the PEC sensor, showing the potential application for detection of real samples.

4. Conclusions

The hybrid photocathode was successfully established by stepwise assembly of CdTe and CNNS as the sensitized PEC materials for

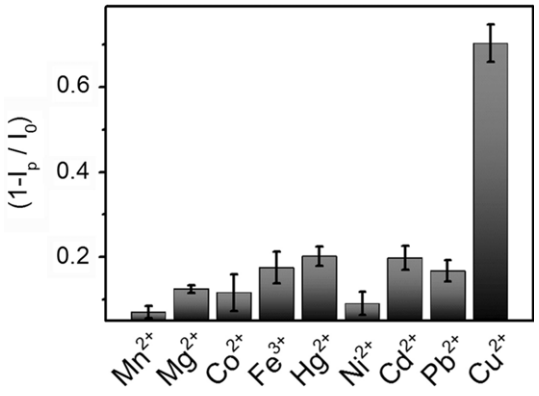

Fig. 7. Quenching efficiency of PEC sensor towards 10 μM Mn^{2+}, Mg^{2+}, Co^{2+}, Fe^{3+}, Hg^{2+}, Ni^{2+}, Cd^{2+}, Pb^{2+} and Cu^{2+}. I_p and I_0 are the photocurrents of hybrid photocathode in the presence and absence of the individual cations, respectively.

photoelectrochemical biosensing. The hybrid photocathode demonstrated an obvious improvement on photocurrent in the absence of exogenous coreactant due to the formation of heterojunction through contact of two semiconductor materials. High photoconversion efficiency in this PEC system can be explained by the extension of electron transit time and electron lifetime. As a model analyte, Cu^{2+} could be selectively adsorbed on both the surface of CdTe and CNNS to decrease the photocurrent. The quenching effect is conducted to the exciton trapping on the surface of CdTe QDs and PET process between CNNS and Cu^{2+}. Based on the dual quenching effect of Cu^{2+}, the hybrid photocathode showed a good performance with a wide linear response range, low detection limit to nanomole and high selectivity, and was successfully achieved the detection of Cu^{2+} in human hair samples. The CNNS-sensitized photocathode provides a good alternative for enhancement of the PEC signal transduction and could be widely used in biosensing and clinical diagnosis.

Acknowledgments

We gratefully acknowledge the National Basic Research Program (2010CB732400) and National Natural Science Foundation of China (21375060, 21135002 and 21121091).

References

[1] R.H. Coridan, K.A. Arpin, B.S. Brunschwig, P.V. Braun, N.S. Lewis, Nano Lett. 14 (2014) 2310–2317.
[2] J.J. Wang, H.F. Sun, J. Huang, Q.X. Li, J.L. Yang, J. Phys. Chem. C 118 (2014) 7451–7457.
[3] J.H. Yang, K. Walczak, E. Anzenberg, F.M. Toma, G.B. Yuan, J. Beeman, A. Schwartzberg, Y.J. Lin, M. Hettick, A. Javey, J.W. Ager, J. Yano, H. Frei, I.D. Sharp, J. Am. Chem. Soc. 136 (2014) 6191–6194.
[4] W.W. Zhao, J.J. Xu, H.Y. Chen, Chem. Rev. 114 (2014) 7421–7441.
[5] C.G. Hu, J.O. Zheng, X.Y. Su, J. Wang, W.Z. Wu, S.S. Hu, Anal. Chem. 85 (2013) 10612–10619.
[6] G.L. Wang, J.J. Xu, H.Y. Chen, Biosens. Bioelectron. 24 (2009) 2494–2498.
[7] W.W. Zhao, Z.Y. Ma, D.Y. Yan, J.J. Xu, H.Y. Chen, Anal. Chem. 84 (2012) 10518–10521.
[8] P.V. Kamat, Acc. Chem. Res. 45 (2012) 1906–1915.
[9] W.J. Wang, Q. Hao, W. Wang, L. Bao, J.P. Lei, Q.B. Wang, H.X. Ju, Nanoscale 6 (2014) 2710–2717.
[10] B.T. Zhang, L.H. Guo, Biosens. Bioelectron. 37 (2012) 112–115.
[11] E. Katz, M. Zayats, I. Willner, F. Lisdat, Chem. Commun. (2006) 1395–1397.
[12] X.R. Zhang, M.S. Liu, H.X. Liu, S.S. Zhang, Biosens. Bioelectron. 56 (2014) 307–312.
[13] W.W. Tu, Y.T. Dong, J.P. Lei, H.X. Ju, Anal. Chem. 82 (2010) 8711–8716.
[14] P.M. Da, W.J. Li, X. Lin, Y.C. Wang, J. Tang, G.F. Zheng, Anal. Chem. 86 (2014) 6633–6639.
[15] V. Subramanian, E.E. Wolf, P.V. Kamat, J. Am. Chem. Soc. 126 (2004) 4943–4950.
[16] X.C. Wang, S. Blechert, M. Antonietti, ACS Catal. 2 (2012) 1596–1606.
[17] C.M. Cheng, Y. Huang, X.Q. Tian, B.Z. Zheng, Y. Li, H. Yuan, D. Xiao, S.P. Xie, M.M. Choi, Anal. Chem. 84 (2012) 4754–4759.
[18] C.M. Cheng, Y. Huang, J. Wang, B.Z. Zheng, H.Y. Yuan, D. Xiao, Anal. Chem. 85 (2013) 2601–2605.
[19] K. Katsumata, R. Motoyoshi, N. Matsushita, K. Okada, J. Hazard. Mater. 260 (2013) 475–482.
[20] E.Z. Lee, Y.S. Jun, W.H. Hong, A. Thomas, M.M. Jin, Angew. Chem. Int. Ed. Engl. 49 (2010) 9706–9710.
[21] S.C. Yan, Z.S. Li, Z.G. Zou, Langmuir 25 (2009) 10397–10401.
[22] Y.J. Zhang, T. Mori, J.H. Ye, M. Antonietti, J. Am. Chem. Soc. 132 (2010) 6294–6295.
[23] L.C. Chen, X.T. Zeng, P. Si, Y.M. Chen, Y.W. Chi, D.H. Kim, G.N. Chen, Anal. Chem. 86 (2014) 4188–4195.
[24] Y.T. Liu, Q.B. Wang, J.P. Lei, Q. Hao, W. Wang, H.X. Ju, Talanta 122 (2014) 130–134.
[25] X.J. She, H. Xu, Y.G. Xu, J. Yan, J.X. Xia, L. Xu, Y.H. Song, Y. Jiang, Q. Zhang, H.M. Li, J. Mater. Chem. A 2 (2014) 2563–2570.
[26] X.L. Zhang, C. Zheng, S.S. Guo, J. Li, H.H. Yang, G. Chen, Anal. Chem. 86 (2014) 3426–3434.
[27] X.H. Li, X.C. Wang, M. Antonietti, Chem. Sci. 3 (2012) 2170.
[28] B. Christiane, P.V.D.E. Frank, R. Michiel, M.B. Anton, G. Marianne, J.S. Jan, A. Wim, Environ. Toxicol. Chem. 22 (2003) 1340–1349.
[29] P. Wang, X.Y. Ma, M.Q. Su, Q. Hao, J.P. Lei, H.X. Ju, Chem. Commun. 48 (2012) 10216–10218.
[30] N. Gaponik, D.V. Talapin, A.L. Rogach, K. Hoppe, E.V. Shevchenko, A. Kornowski, A. Eychmüller, H. Weller, J. Phys. Chem. B 106 (2002) 7177–7185.
[31] X.D. Zhang, X. Xie, H. Wang, J.J. Zhang, B.C. Pan, Y. Xie, J. Am. Chem. Soc. 135 (2013) 18–21.
[32] W.W. Yu, L.H. Qu, W.Z. Guo, X.G. Peng, Chem. Mater. 15 (2003) 2854–2860.
[33] L. Bao, L.F. Sun, Z.L. Zhang, P. Jiang, F.W. Wise, H.D. Abruña, D.W. Pang, J. Phys. Chem. C 115 (2011) 18822–18828.
[34] W.W. Zhao, S. Shan, Z.Y. Ma, L.N. Wan, J.J. Xu, H.Y. Chen, Anal. Chem. 85 (2013) 11686–11690.
[35] J. Wang, I. Mora-Sero, Z.X. Pan, K. Zhao, H. Zhang, Y.Y. Feng, G. Yang, X.H. Zhong, J. Bisquert, J. Am. Chem. Soc. 135 (2013) 15913–15922.
[36] J.Q. Tian, Q. Liu, A.M. Asiri, A.O. Al-Youbi, X.P. Sun, Anal. Chem. 85 (2013) 5595–5599.
[37] Q.M. Shen, X.M. Zhao, S. Zhou, W.H. Hou, J.J. Zhu, J. Phys. Chem. C 115 (2011) 17958–17964.